



## Measurement of Natural Radioactivity Levels and Evaluation of Radiological Hazard Risks in Areas of Eastern Coastline Sediments of Lake Hawassa in Ethiopia's Sidama Region

Messele Kebede Kassa✉ | Tilahun Tesfaye Deressu

Department of Physics, Addis Ababa University, Arat Kilo Campus, Fax: +251-111-239768, P.O.Box: 1176, Addis Ababa, Ethiopia.

### Article Info

**Article type:**  
Research Article

**Article history:**  
Received: 23 Mar 2023  
Revised: 03 Jul 2023  
Accepted: 06 Nov 2023

**Keywords:**  
*Sediment;*  
*Natural radioactivity*  
*Radiological hazard index*  
*Lake Hawassa*  
*Ethiopia*

### ABSTRACT

Natural radioactivity levels in the eastern coastline of Lake Hawassa sediment samples of Ethiopia's Sidama Region have been measured. Sediment samples were collected and analyzed using gamma-ray spectrometry (high purity germanium detector) to evaluate the radioisotopes of  $^{238}\text{U}$  ( $^{214}\text{Pb}$ ,  $^{214}\text{Bi}$ ),  $^{232}\text{Th}$  ( $^{228}\text{Ac}$ ,  $^{212}\text{Pb}$ ), and  $^{40}\text{K}$  and their ranges of activity concentrations were 11.70 to 29.73  $\text{Bq kg}^{-1}$ , 19.01 to 58.61  $\text{Bq kg}^{-1}$ , and BDL to 827.21  $\text{Bq kg}^{-1}$ , with average values of  $16.51 \pm 1.20 \text{ Bq kg}^{-1}$ ,  $28.17 \pm 2.27 \text{ Bq kg}^{-1}$ , and  $673.95 \pm 29.92 \text{ Bq kg}^{-1}$  (dry mass), respectively. The radiological hazard indices average values (radium equivalent ( $R_{eq}$ ) ( $108.69 \text{ Bq kg}^{-1}$ ); hazard index ( $H_{ex}$ ) (0.29); excess lifetime cancer risk (ELCR) ( $0.23 \times 10^{-3}$ ); absorbed dose rate ( $D_R$ ) ( $52.70 \text{ nGy h}^{-1}$ ); annual effective dose equivalent (AEDE) ( $0.07 \text{ mSv yr}^{-1}$ ); and annual gonadal dose equivalent (AGDE) ( $0.38 \text{ mSv yr}^{-1}$ ) were also evaluated and compared to the worldwide-recommended values. All results of radiological hazard indices obtained in this study were lower than their worldwide-recommended values were  $370 \text{ Bq kg}^{-1}$ ,  $\leq 1$ ,  $59 \text{ nGy h}^{-1}$ ,  $0.07 \text{ mSv yr}^{-1}$ ,  $0.29 \times 10^{-3}$ , and  $0.3 \text{ mSv yr}^{-1}$  of radium equivalent activity, external hazard index, outdoor absorbed dose rate, outdoor annual effective dose equivalent, excess lifetime cancer risk, and annual gonadal dose equivalent, respectively. This suggests the eastern coastline of Lake Hawassa is safe from radioactive risk for aquatic species and various human activities, and appears as essential radiometric baseline information for further environmental monitoring programs.

**Cite this article:** Kebede Kassa, M., & Tesfaye Deressu, T. (2023). Measurement of Natural Radioactivity Levels and Evaluation of Radiological Hazard Risks in Areas of Eastern Coastline Sediments of Lake Hawassa in Ethiopia's Sidama Region. *Pollution*, 9 (4), 1819-1837.  
<https://doi.org/10.22059/poll.2023.357027.1843>



© The Author(s).

Publisher: University of Tehran Press.

DOI: <https://doi.org/10.22059/poll.2023.357027.1843>

## INTRODUCTION

Humans regularly expose to ionizing radiations, which are naturally found in various environmental media. Natural environmental radioactivity is primarily produced by radioactive nuclides from the  $^{232}\text{Th}$  and  $^{238}\text{U}$  series and primordial radionuclides like  $^{40}\text{K}$ . These radioactive elements are found in varying concentrations in soils, rocks, plants, sand, water, and building materials, depending on the geology and geography of the area. Natural radiation from these natural sources is responsible for approximately 87 percent of human radiation exposure and radiation caused by humans contributes for the remainder (UNSCEAR, 2000; Shetty and Narayana, 2010; Ugbede and Akpolile, 2019). Humans should therefore be aware of the radiation impacts caused by naturally occurring and artificially produced radioactive materials

\*Corresponding Author Email: [mesele.kebede@aau.edu.et](mailto:mesele.kebede@aau.edu.et)

in their environment. Radon and its decay products, which are found in soil, sediment, and construction materials, mostly cause internal radiation exposure, which affects the respiratory tract (Hameed et al., 2014). Long-term inhalation exposure to uranium and radium can have a number of adverse health effects, including anemia, acute leucopenia, chronic lung diseases, and mouth necrosis. Nasal, cranial, and bone tumors are all brought on by exposure to Radium. Leukemia, lung, pancreatic, hepatic, skeletal, and kidney malignancies are all brought on by exposure to thorium (Ramasamy et al., 2011).

Sands and silts produced by the weathering and erosion of rock and soil make up the majority of sediments that settle in. Therefore, the distribution of natural radioactivity in the aquatic ecosystem of the lake is important to research. Sediment samples collected from these lake basins provide an insight of the typical activity of neighboring geographic areas (Eroğlu and Kabadayi, 2013).

Radioactive contamination could possibly have been measured in sediment's environment since it not only works as the primary source of human continuous radiation exposure but also facilitates the migration of radionuclides into biological systems (Ramasamy et al., 2011; Suresh et al., 2011). Sediment contamination with radioactive nuclides from the  $^{238}\text{U}$  and  $^{232}\text{Th}$  decay series, as well as naturally occurring  $^{40}\text{K}$ , is particularly important from a radiological standpoint because the radionuclides radioactivity levels measured in the contaminated sediment are useful for reducing the harmful effects of ionizing radiation on the environment and human health (Botwe et al., 2016).

Lake Hawassa is one of the main basins of lakes in the Ethiopian Rift Valley, which is used significantly for irrigation of agriculture, public consumption by certain city dwellers and others who live in nearby rural areas, entertainment, watering cattle, and fish aquaculture (Semaria Moga et al., 2021). The lake has a surface area of roughly 92 km<sup>2</sup>, measures 16 km in length and up to 8 km in width, and has an approximate capacity of 1.3 billion m<sup>3</sup>. The lake has an utmost depth of 22 meters and an average depth of 11 meters. It is home to a variety of fish, birds, and large creatures like hippopotamuses. Furthermore, Amora Gedel's coastline features a small fish market (Tarekegn and Seyoum, 2020).

The lake's effect is mainly shown in the water quality, which is not adequate for cultivation, consumption, aquatic organisms, or entertainment purposes and was primarily caused by man-made activities in its drainage basin. The residential waste materials are delivered into drainage, roads, and the lake, and the leftover fish fragments are also thrown in every corner around the lake. As a result, sanitation is a major problem, and generally, the city does not have enough management mechanisms for waste materials and public latrines. Additionally, larger commercial buildings offer traditional washing systems but no wastewater treatment, and everywhere in and around the Hawassa city areas, large building construction has taken place. Due to this, building materials such as sediment, cement, concrete, and others runoff from rain to the lake. The Tikur-Wuha River, which gave its name to a little marshy tract that supplied Lake Hawassa, is also known to discharge effluents into streams and rivers from commercial and industrial pollution sources such as the BGI, Moha soft drink, flour, and ceramic factories. Moreover, the referral hospital and Hawassa Industrial Park discharge their effluents into the lake. This is a threat to the survival of aquatic creatures as well as to the people who rely on rivers, tributaries, and lakes for residential and other purposes (personal observation) and (Semaria Moga et al., 2021). The effects of this phenomenon were also seen in phenomena like livestock deaths and a decline in the quality of vegetables grown with irrigation (Tarekegn and Seyoum, 2020).

Accordingly, estimating environmental radiation doses under this study is very crucial, as is evaluating the population's health hazards and it provides a baseline for monitoring changes in environmental radioactivity brought on by anthropogenic activities.

In recent years, there has been a lot of effort put into measuring and evaluating natural

radioactivity levels in lake sediments and river sediments in various parts of the world. For instance, in lake sediments such as Egypt (Ibrahim et al., 1995; Khater et al., 2005); Turkey (Eroğlu and Kabadayi, 2013; Erenturk et al., 2014; Kobya et al., 2015); Nigeria (Isinkaye and Emelue, 2015); Ghana (Darko et al., 2017); and river sediments such as Egypt (El-Gamal et al., 2007); Turkey (Kurnaz et al., 2007); India (Suresh et al., 2011; Ramasamy et al., 2011; Murugesan et al., 2015); Nigeria (Jibiri and Okeyode, 2012; Ugbede and Akpolile, 2019); Pakistan (Qureshi et al., 2014); Brazil (Da Silva and Da Silva Filho, 2019); China (Lu et al., 2008) and Bangladesh (Chowdhury et al., 1999). Consequently, there is no information available at this time regarding the radioactive levels of  $^{238}\text{U}$ ,  $^{232}\text{Th}$ , and  $^{40}\text{K}$  in Lake Hawassa sediment.

In previous years, Hawassa City was one of the Ethiopia's fastest-growing cities, with an approximate 4% annual growth rate (Mulugeta et al., 2021); the coastline of Lake Hawassa has seen an increase in urbanization for socioeconomic purposes, including tourism, fishing, irrigation for farming, entertainment, and resorts (personal observation) and (Semaria Moga et al., 2021). As a result, measuring the natural radioactivity levels of sediment samples is essential to establishing a scientific database of the radioactive background levels, identifying the radiological effects of places where people regularly partake in diverse activities, and determining any unintentional contamination of the eastern coastline of Lake Hawassa.

This study's objective is to measure the levels of naturally occurring radioactivity ( $^{238}\text{U}$  (uranium),  $^{232}\text{Th}$  (thorium), and  $^{40}\text{K}$  (potassium)) in sediments collected from specific locations of eastern Lake Hawassa, Sidama Region, Ethiopia, where people regularly partake in diverse activities. The radium equivalent activity (Raeq), hazard index (external ( $H_{\text{ex}}$ )), excess lifetime cancer risk (ELCR), absorbed dose rate ( $D_{\text{R}}$ ), annual effective dose equivalent (AEDE), and annual gonadal dose equivalent (AGDE) were evaluated and compared to previous study results. The findings of this study will also provide background information on natural radioactive isotopes, very crucial radiometric baseline data for future environmental monitoring programs, and awareness to people involved in diverse activities near the eastern Lake Coastline and visiting tourists at the lake.

## MATERIALS AND METHODS

One of the eight lakes in the Ethiopian Rift Valley, Lake Hawassa has a shoreline that extends for roughly 55 km, which is the smallest of the other natural lakes in the central Rift Valley. It is embraced by many mountains, including Mt. Tabor and Mt. Alamura, which are 1810 and 2019 meters above sea level, respectively, and is located 275 kilometers south of the capital city, Addis Ababa, and west of Hawassa town (Menberu et al., 2021). It includes five sub-watersheds: Dorebafena-Shamena, Wedesa-Kerama, TikurWuha, Lalima-Wendo Kosha, and Shashemene-Toga. The sub-geographic basin's coordinates are  $6^{\circ}45'$  to  $7^{\circ}15'$  N and  $38^{\circ}15'$  to  $38^{\circ}45'$  E, respectively. The sub-basin crosses two regions, two zones, and twelve weredas. Overall, 71% of the sub-basin is within the Sidama Regional State, and 22% within the administrative boundary areas of the Oromiya Regional State. Lake Hawassa is located in both regions, contributing the remaining 7%. The Hawassa sub-basins have a population of 158,275 at Hawassa city, and its mean annual rainfall varies from 950 to 1400 mm, with an average of 959 mm, and its average yearly temperature is  $18.5^{\circ}\text{C}$ ; its daily maximum temperature ranges from  $19$  to  $21^{\circ}\text{C}$ ; and its daily lowest temperature ranges from  $13$  to  $17^{\circ}\text{C}$  (Mulugeta et al., 2021).

The seven sampling sites along the eastern coastline of Lake Hawassa, Sidama Region, Ethiopia, were selected with care to represent areas where people are engaged in diverse activities (Onjefu et al., 2017), that is, engaging in a variety of practices regularly, such as recreation, fishing, fish sales, eating raw fish, washing clothes, taking a bath, and farming vegetables (personal observation).

In the first week of June 2021, seven samples from the lake's surface sediment at a depth

of about 10 cm were purposefully collected with a stainless steel trowel in a single day at the lake's inner side, 50 cm from the lake's coastline, at sample site intervals of 2.5 to 3 km, and 1.5 kg were weighed from each site sample along the lake's coastline to maintain consistency in sampling (Ravisankar et al., 2014). The distance spanned about 40% of 55km the lake's coastline. Grass, leaves, roots, and small pieces of wood were hand-removed and placed in a polyethylene bag with labels for subsequent laboratory analysis identification. The seven surface sediment samples were represented by twenty-eight sub-samples across all eastern coastline interval sites, which were collected as four sub-samples per interval site. As shown in Fig.1 and Table 1 columns 1 and 2, the seven successive sampling sites (SDS01 to SDS07)

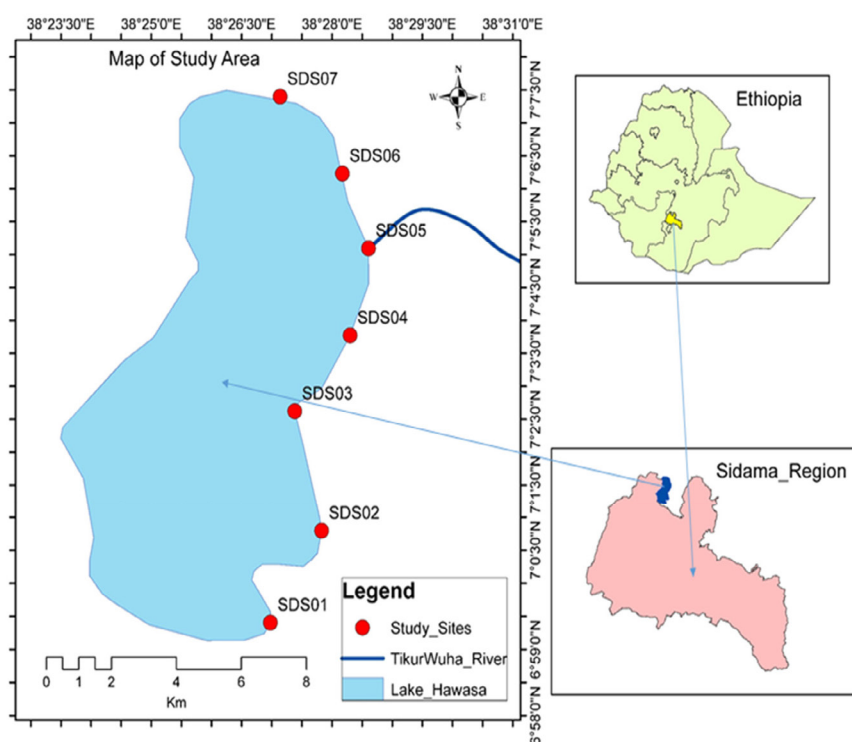


Fig. 1. The study sites of Lake Hawassa on a map.

Table 1. Shows that for Lake Hawassa, activity concentrations of radionuclides  $^{238}\text{U}$ ,  $^{232}\text{Th}$ , and  $^{40}\text{K}$  in sediment samples measured.

Coordinates of location (GPS)		Sample code	No. of samples per site interval	$^{238}\text{U}$ ( $\text{Bq kg}^{-1}$ )	$^{232}\text{Th}$ ( $\text{Bq kg}^{-1}$ )	$^{40}\text{K}$ ( $\text{Bq kg}^{-1}$ )
Latitude (N)	Longitude (E)			$^{238}\text{U} \pm \text{SD}^a$	$^{232}\text{Th} \pm \text{SD}^a$	$^{40}\text{K} \pm \text{SD}^a$
6° 59' 28.03"	38° 26' 57.61"	SDS01	4	11.92 ± 0.87	20.07 ± 1.64	826.41 ± 36.24
7° 00' 52.83"	38° 27' 50.86"	SDS02	4	29.73 ± 2.01	58.61 ± 4.60	804.83 ± 35.64
7° 02' 36.38"	38° 27' 22.26"	SDS03	4	15.01 ± 1.18	25.45 ± 2.02	BDL <sup>b</sup>
7° 03' 50.33"	38° 28' 20.45"	SDS04	4	17.03 ± 1.30	27.17 ± 2.22	770.36 ± 34.93
7° 05' 11.20"	38° 28' 35.24"	SDS05	4	17.74 ± 1.27	27.05 ± 2.21	673.73 ± 30.59
7° 06' 14.31"	38° 28' 07.63"	SDS06	4	12.45 ± 0.89	19.01 ± 1.56	827.21 ± 36.27
7° 07' 26.29"	38° 27' 07.47"	SDS07	4	11.70 ± 0.88	19.83 ± 1.62	815.10 ± 35.74
Average				16.51 ± 1.20	28.17 ± 2.27	673.95 ± 29.92
Maximum				29.73 ± 2.01	58.61 ± 4.60	827.21 ± 36.27
Minimum				11.70 ± 0.88	19.01 ± 1.56	BDL <sup>b</sup>

<sup>a</sup> Standard deviation

<sup>b</sup> Below the detection limits

were located at latitudes of 6° 59' 28.03" and 7° 07' 26.29" N and longitudes of 38° 26' 57.61" and 38° 27' 07.47" E.

For gamma-ray spectrometry analysis purposes, samples were ground and sieved using a 2 mm mesh sieve to homogenize and pulverize them. The sediments were then oven-dried for 10 hours at 100 degrees Celsius until they reached a consistent weight. After that, they were weighed at 500 grams each. Then, they were kept into 500mL Marinelli beakers of uniform size and sealed for 30 days to achieve radioactive equilibrium, in which the daughters' decay rate equaled the parent's (Karahana and Bayulken, 2000). The  $^{238}\text{U}$  activity was supposed to be represented by the activities of  $^{214}\text{Pb}$  and  $^{214}\text{Bi}$  when they were in equilibrium with their parents, while the  $^{232}\text{Th}$  activity was assumed to be represented by the activities of  $^{228}\text{Ac}$  and  $^{212}\text{Pb}$ . The average values of their progeny,  $^{214}\text{Pb}$ ,  $^{214}\text{Bi}$  and  $^{228}\text{Ac}$ ,  $^{212}\text{Pb}$ , were used to compute the activities of  $^{238}\text{U}$  and  $^{232}\text{Th}$ , respectively (Tzortzis et al., 2004). Ethiopia's Radiation Protection Authority, Addis Ababa, Ethiopia, was responsible for all radioactivity measurements by means of gamma-ray spectrometry (HPGe detector).

#### *Energy and efficiency calibration of gamma-ray spectrometry (HPGe detector)*

A gamma ray spectrometer detector with a 57.5 mm diameter and 51.5 mm thick crystals was used for gamma spectrometry analysis. The operating voltage was +2800V, the relative efficiency was 70.0 percent, the energy resolution was 1.9 keV, and the FWHM was 1.33MeV.

The spectra were analyzed with Canberra's Genie-2000 software, version 3.0. To minimize interference from background radiation from terrestrial and extraterrestrial sources in the measured spectrum, the detector was surrounded with a cylindrical lead shield with a fixed bottom and adjustable cover.

In our present study, the background distribution of an empty Marinelli beaker (500 ml) was measured under identical conditions as a sample measurement. A total of 28,800 seconds, or 8 hours, passed throughout the identical geometry measurement.

The background radiation was removed after the measurement to ascertain the naturally occurring background distribution in the environment surrounding the detector. Marinelli calibration sources including Am (59.54 keV), Cd (88.040 keV), Co (122.061 keV and 136, 474 keV), Sn (391.698 keV), Sr (514.007 keV), Cs (661.657 keV), Y (898.042 and 1836.063 keV), and Co (1173.22 and 1332.492 keV) were used to calibrate the spectrometer's energy and relative efficiency.

Each sample data was counted for 28,800 seconds, or 8 hours to determine the activities of  $^{238}\text{U}$ ,  $^{232}\text{Th}$ , and  $^{40}\text{K}$ . The specific activity of  $^{238}\text{U}$  was determined using gamma-ray lines of  $^{214}\text{Bi}$  at 609.31, 1120.29, and 1764.49 keV and  $^{214}\text{Pb}$  at 295.21, and 351.92 keV decay products, whereas the specific activity of  $^{232}\text{Th}$  was measured using gamma-ray lines of  $^{228}\text{Ac}$  at 968.97, and 911.21 keV; and  $^{212}\text{Pb}$  at 77.11 keV, and 238.63 decay products and the specific activity of  $^{40}\text{K}$  was directly determined from its gamma-ray line at 1460.81 keV (Onjefu et al., 2017). The determined values for the below detection limits (BDL) for  $^{238}\text{U}$ ,  $^{232}\text{Th}$ , and  $^{40}\text{K}$  were  $0.75 \text{ Bq kg}^{-1}$ ,  $2.20 \text{ Bq kg}^{-1}$ , and  $21.8 \text{ Bq kg}^{-1}$ , respectively.

#### *Theoretical calculation of activity concentrations and radiological hazard metrics*

The concentrations of activity were obtained by measuring the decay products (Kurnaz et al., 2007). The sample's net count was obtained by subtracting a linear background distribution of the appropriate peak energy region from the sample's total count. Equation (1) was used to calculate the activity concentrations ( $\text{Bq kg}^{-1}$ ) in the study sample (Fares, 2017):

$$A = \frac{(CPS)_{net}}{I \epsilon M} \quad (1)$$

Where  $A$  is the activity concentration in  $\text{Bq kg}^{-1}$ , ( $\text{CPS}$ )<sub>net</sub> is (count per second). ( $I$ ) is the intensity of the gamma ray-line in a radionuclide,  $\epsilon$  is the efficiency detector for each gamma ray-line and  $M$  is the mass of the sample in kilograms.

The radium equivalent activity ( $Ra_{eq}$ ) is a typical radiological index for comparing the particular activities of materials containing  $^{238}\text{U}$ ,  $^{232}\text{Th}$ , and  $^{40}\text{K}$  by a single quantity. Equation (2) was assumed using the premise that  $370 \text{ Bq kg}^{-1}$  of  $^{238}\text{U}$ ,  $259 \text{ Bq kg}^{-1}$  of  $^{232}\text{Th}$ , and  $4810 \text{ Bq kg}^{-1}$  of  $^{40}\text{K}$  produce an identical gamma radiation dose rate. The weighted total of the activity of  $^{238}\text{U}$ ,  $^{232}\text{Th}$ , and  $^{40}\text{K}$  is the radium equivalent (Beretka and Mathew, 1985; Botwe et al., 2016; Ugbede and Akpolile, 2019) equation (2) was used to calculate radium equivalent activity ( $Ra_{eq}$ ).

$$Ra_{eq} = A_U + 1.43A_{Th} + 0.077A_K \quad (2)$$

Where  $A_U$ ,  $A_{Th}$  and  $A_K$  are the activity concentrations of  $^{238}\text{U}$ ,  $^{232}\text{Th}$  and  $^{40}\text{K}$  in  $\text{Bq kg}^{-1}$ , respectively. The radium equivalent activity ( $Ra_{eq}$ ) must have a minimum value of less than  $370 \text{ Bq kg}^{-1}$ , which is equivalent to a dose limit of  $1.00 \text{ mSv yr}^{-1}$  for the general public (ICRP, 2007; UNSCEAR, 2008).

External gamma ray exposure causes external hazard ( $H_{ex}$ ), which is a radiation hazard risk. Equation (3) was used to determine the external hazard index ( $H_{ex}$ ) (Darwish et al., 2015; Darko et al., 2017).

$$H_{ex} = \frac{A_U}{370\text{Bq.kg}^{-1}} + \frac{A_{Th}}{259\text{Bq.kg}^{-1}} + \frac{A_K}{4810\text{Bq.kg}^{-1}} \quad (3)$$

$370 \text{ Bq kg}^{-1}$  of  $^{238}\text{U}$ ,  $259 \text{ Bq kg}^{-1}$  of  $^{232}\text{Th}$ , and  $4810 \text{ Bq kg}^{-1}$  of  $^{40}\text{K}$  are assumed to provide an identical gamma dose rate (Karahana and Bayulken, 2000). External exposure to uranium-238, thorium-232 and its decay products and natural potassium-40 is regulated by the external hazard index ( $H_{ex}$ ), which, according to UNSCEAR (2000) (UNSCEAR, 2000), must be less than unity for the radioactive risk to be considered minimal. The main goal of  $H_{ex}$  is to keep the radiation exposure below the  $1\text{mSv yr}^{-1}$  dose equivalent limit for public (ICRP, 2007; UNSCEAR, 2008). As a result, for the radiation hazards to be minimal, their values must be less than unity. For the radiation hazard to be insignificant, the values of the hazard index  $H_{ex}$  must be less than unity (Darwish et al., 2015).

The radiation absorbed dose rate in air at 1.0 m above ground level was calculated using conversion factors of 0.462, 0.604, and 0.0417 for  $^{238}\text{U}$ ,  $^{232}\text{Th}$ , and  $^{40}\text{K}$  in  $\text{nGy h}^{-1}$  per  $\text{Bq kg}^{-1}$  respectively (Beretka & Mathew, 1985; Qureshi et al., 2014; Botwe et al., 2016; Ugbede and Akpolile, 2019) as equation (4).

$$D_{R_{out}} (\text{nGyh}^{-1}) = 0.462A_U + 0.604A_{Th} + 0.0417A_K \quad (4)$$

Where  $A_U$ ,  $A_{Th}$  and  $A_K$  are the activity concentration of  $^{238}\text{U}$ ,  $^{232}\text{Th}$  and  $^{40}\text{K}$  in  $\text{Bq kg}^{-1}$ , respectively.

To convert outdoor absorbed dose ( $D_{R_{out}}$ ) in air to effective dose, the outdoor annual effective dose equivalent ( $AEDE_{out}$ ) was calculated. According to UNSCEAR (2000) (UNSCEAR, 2000), the conversion coefficient from absorbed radiation in the air to effective dose received by adults is  $0.7 \text{ Sv Gy}^{-1}$ . The outdoor occupancy factor is 0.2. The annual effective dose equivalent was estimated using equation (5) (Erenturk et al., 2014; Qureshi et al., 2014; Botwe et al., 2016; Onjefu et al., 2017).

$$AEDE_{out} (\text{mSvyr}^{-1}) = D_{R_{out}} (\text{nGyh}^{-1}) \times 8760\text{hyr}^{-1} \times 0.2 \times 0.7\text{SvGy}^{-1} \times 10^{-6} \quad 5 \quad (5)$$

Where  $D_{eff}$  is the annual effective dose in  $mSvyr^{-1}$ ,  $D_o$  is the air absorbed dose rate, and 8760 is the annual number of hours. The conversion factor of  $0.7 Sv Gy^{-1}$  between the absorbed dose in air and the effective dose received by adults (UNSCEAR, 2000) and an approximate 20 percent of outdoor time are all included in Eq. (5) along with the dose rate data derived from the concentration values of naturally occurring radionuclides in sediment ( $D_o$ ).

Using the equation (6), the excess lifetime cancer risk (ELCR) was calculated from the annual effective dose equivalent (Qureshi et al., 2014; Murugesan et al., 2015; Onjefu et al., 2017; Ugbede and Benson, 2018; Ugbede and Akpolile, 2019).

$$ELCR_{out} = AEDE_{out} \times DL \times RF \quad (6)$$

Where  $DL$  and  $RF$  are the duration of life (70 years), and risk factor ( $0.05 Sv^{-1}$ ), respectively. Defined the risk factor as fatal cancer risk per sievert is assigned a value of 0.05 by ICRP-103 (2007) and ICRP-106 (2008) recommendations (ICRP, 2007; UNSCEAR, 2008) for the public for random effects, for low-level radiations.

Annual gonadal dose equivalent ( $AGDE$ ) is a metric for the genetic significance of the yearly dose equivalent received by the reproductive organs (gonads) of the population (Ramasamy et al., 2014; Ugbede and Akpolile, 2019). As a result, the annual gonadal dose equivalent ( $AGDE$ ) due to the particular activities of  $^{238}U$ ,  $^{232}Th$ , and  $^{40}K$ , as well as conversion factors of 3.09, 4.18, and  $0.314 Svyr^{-1}$  per  $Bq kg^{-1}$ , was calculated by equation (7) (Morsy et al., 2012; Botwe et al., 2016; Ugbede and Akpolile, 2019).

$$AGDE (mSvyr^{-1}) = 3.09A_U + 4.18A_{Th} + 0.314A_K \quad (7)$$

Where  $AGDE$  stands for annual gonadal dose equivalent,  $A_U$ ,  $A_{Th}$  and  $A_K$  are the activity concentration of  $^{238}U$ ,  $^{232}Th$  and  $^{40}K$  respectively.

## RESULTS AND DISCUSSION

The distribution of  $^{238}U$ ,  $^{232}Th$ , and  $^{40}K$  in the sediment samples, as well as their activity concentrations, are presented in Table 1 and Fig.2. The results show that seven sequential locations (SDS 01 up to SDS 07) along Lake Hawassa coastline contained varying concentrations of these natural radionuclides.

The table compares the activity concentrations of  $^{238}U$  in the seven locations, and it can be seen that the lake's SDS02 site had the highest activity concentration ( $29.73 \pm 2.01 Bq kg^{-1}$ ), while SDS01 site had the lowest activity concentration ( $11.92 \pm 0.87 Bq kg^{-1}$ ); with an average value of  $16.51 \pm 1.20 Bq kg^{-1}$ . The lake's SDS02 site ( $58.61 \pm 4.60 Bq kg^{-1}$ ) and SDS06 site ( $19.01 \pm 1.56 Bq kg^{-1}$ ) had the highest and lowest activity concentrations of  $^{232}Th$ , respectively, with an average value of  $28.17 \pm 2.27 Bq kg^{-1}$ . The average activity concentrations of  $^{238}U$  and  $^{232}Th$  were lower than the worldwide averages (the worldwide average for these radionuclides are 33 and 45  $Bq kg^{-1}$ , respectively (UNSCEAR, 2008). For  $^{40}K$ , the lake's SDS06 site had the highest value ( $827.21 \pm 36.27 Bq kg^{-1}$ ) and SDS03 site (BDL) the lowest value, with an average value of  $673.95 \pm 29.92 Bq kg^{-1}$ . The activity concentrations of  $^{40}K$  in all sites were higher than the worldwide averages (the worldwide average for this radionuclide is 420  $Bq/kg$ ), except at the SDS03 site (BDL), which had the lowest activity concentration (UNSCEAR, 2008). The high monazite content in the lake's SDS02 sampling site area may have caused an increase in the concentration of  $^{232}Th$  (Orgun, et al., 2007), while the solubility and mobility of  $U(VI)O_2^{2+}$  in the sediments at this lake site may have caused a decrease in  $^{238}U$  (Powell et al., 2007). A rise in loamy and clayey sediments in the area may be the cause of the  $^{40}K$  concentration's rising



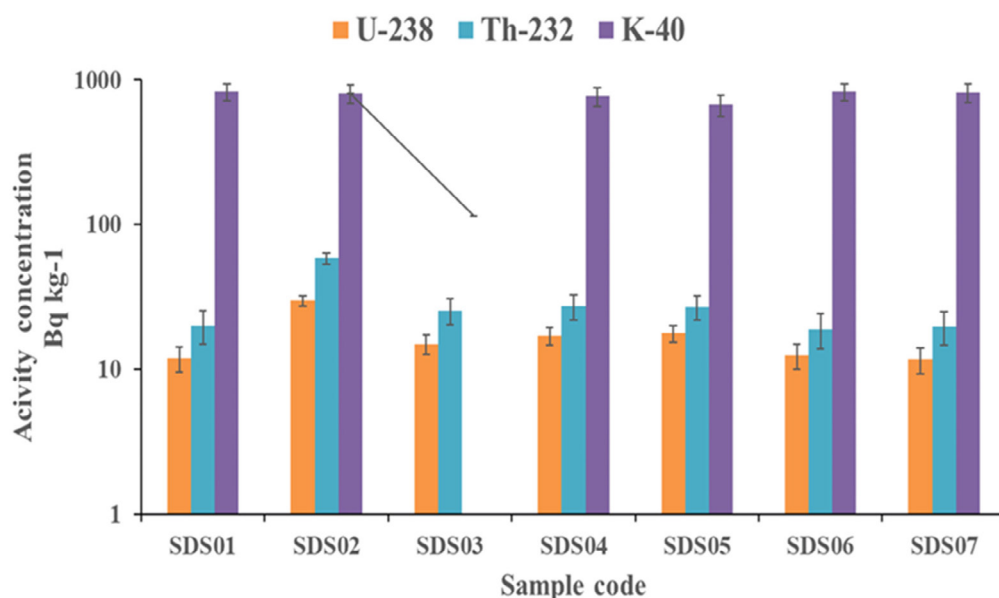


Fig. 2. Illustrates activity concentrations of <sup>238</sup>U, <sup>232</sup>Th, and <sup>40</sup>K in Lake Hawassa with sediment sample codes.

trend at the SDS06 sampling site of the lake (El-Gamal et al., 2007).

In the sediment samples, <sup>40</sup>K had the highest average activity, followed by <sup>232</sup>Th and <sup>238</sup>U (<sup>40</sup>K > <sup>232</sup>Th > <sup>238</sup>U). A similar pattern has been found in the sediments of Lake Nasser, Egypt (Ibrahim et al., 1995); Altikaya Dam Lake and Derbent Dam Lake, Turkey (Eroğlu and Kabadayi, 2013); Borcka Dam Lake and Murath Dam Lake, Turkey (Kobyas et al., 2015); and Oguta Lake, South East Nigeria (Isinkaye and Emelue, 2015) (see Table 2). Due to the limited geochemical mobility and insoluble nature of thorium in water, the activity of <sup>232</sup>Th was found to be higher than that of <sup>238</sup>U in all sediment samples (Suresh et al., 2011; Isinkaye and Emelue, 2015). The wide range in activity concentration values can also be attributed to the marine environment's physical, chemical, and geochemical characteristics (El Mamoney and Khater, 2004; SureshGandhi et al., 2014). It also shows how physical and geochemical processes affect the accumulation of radionuclides in the Lake's sediment. The overall activity concentration (<sup>238</sup>U + <sup>232</sup>Th + <sup>40</sup>K) ranges from 40.46 to 893.17 Bq kg<sup>-1</sup>, with an average of 718.63 Bq kg<sup>-1</sup>. This value falls behind that of the sediments of Oguta Lake, South East Nigeria (Isinkaye and Emelue, 2015), Tuomo River Sediments in Burutu, Delta State, Nigeria (Ugbede and Akpolile, 2019), and the São Francisco River sediments in Petrolina, Brazil (Da Silva and Da Silva Filho, 2019) (see Table 2 and Fig.3). The contributions of <sup>238</sup>U, <sup>232</sup>Th, and <sup>40</sup>K to the total activity concentration of the sediments are 2.3 percent, 3.9 percent, and 93.8 percent, respectively, with <sup>40</sup>K contributing the most and, as is typical in soil, the concentration of <sup>40</sup>K activity predominates over the concentrations of <sup>232</sup>Th and <sup>238</sup>U elemental activities (Erenturk et al., 2014).

The activity concentration of the three natural radionuclides are compared in Table 2 and Fig.3 to values found in rivers and lakes from other countries that were studied by other researchers. The comparison of our study with other studies may be helpful in understanding the distribution of radioactivity across different continents and may support world baseline data from Ethiopia as one of the larger African nations.

The average radionuclide concentrations of <sup>238</sup>U, <sup>232</sup>Th, and <sup>40</sup>K reported here are higher than those found in sediments from Ghana's Lake Bosomtwe (Darko et al., 2017), Turkey's Deriner Dam Lake and Borcka Dam Lake (Kobyas et al., 2015), Egypt's Nile River (El-Gamal et al., 2007), and Nigeria's Ogun River, Southwestern (Jibiri and Okeyode, 2011, 2012). This study's



**Table 2.** Compares the average activity concentrations of  $^{238}\text{U}$ ,  $^{232}\text{Th}$ , and  $^{40}\text{K}$  in Lake Hawassa sediment from rivers and lakes in various countries.

Country	River/ Lake	Average activity concentration ( $\text{Bq kg}^{-1}$ )			References
		$^{238}\text{U}$	$^{232}\text{Th}$	$^{40}\text{K}$	
Brazil	São Francisco River	31.54	200.15	1023	(Da Silva and Da Silva Filho, 2019)
Bangladesh	Shango River	25.4	57.5	255	(Chowdhury et al., 1999)
	Karnaphuli River	37.9	65.5	272	
China	Wei River	21.8	33.1	833.3	(Lu et al., 2008)
Egypt	Lake Nasser	20.6	23	154.5	(Ibrahim et al., 1995)
	Nile River	16.3	12.94	200.21	(El-Gamal et al., 2007)
Ghana	Lake Bosomtwe	7.9	7.83	169.73	(Darko et al., 2017)
Nigeria	Oguta Lake	47.89	55.37	1023	(Isinkaye and Emelue, 2015)
	Ogun River	12.6	11.8	499.5	(Jibiri and Okeyode, 2011)
		12.65	11.78	499.48	(Jibiri and Okeyode, 2012)
Pakistan	Tuomo River	43.89	99.21	793.99	(Ugbede and Akpolile, 2019)
	Hunza, Gilgit and Indus River	50.66	70.15	531.7	(Qureshi et al., 2014)
India	Ponnaiyar River	6.43	52.76	395.6	(Ramasamy et al., 2011)
	Ponnaiyar River	7.31	46.85	384.113	(Suresh et al., 2011)
	Palar River	9.81	36.49	742.46	(Murugesan et al., 2015)
Turkey	Altinkaya Dam Lake	19.5	27.7	460	(Eroğlu and Kabadayi, 2013)
	Derbent Dam Lake	18.8	25.5	365	
	Lake Van (average of Upper and depth)	199.5	66.5	374.5	(Erenturk et al., 2014)
	Deriner Dam Lake	15.8	13.9	551.5	(Kobyas et al., 2015)
	Borecka Dam Lake	3.7	12.5	473.8	
Murath Dam Lake	14.4	30	491.7		
	Firtina River	39	38	573	(Kurnaz et al., 2007)
Previous studies range		3.7-199.5	7.83-200.15	154.5-1023	
Ethiopia	Lake Hawassa	16.51	28.17	673.95	Present study
Worldwide-recommended values		33	45	420	(UNSCEAR, 2008)

average value of  $673.95 \text{ Bq kg}^{-1}$  for  $^{40}\text{K}$  is lower than the  $1023 \text{ Bq kg}^{-1}$  value found in Oguta Lake sediments in Nigeria (Isinkaye and Emelue, 2015); the  $793.99 \text{ Bq kg}^{-1}$  value found in the Tuomo River in Nigeria (Ugbede and Akpolile, 2019); and the  $742.46 \text{ Bq kg}^{-1}$  value found in the Palar River in India (Murugesan et al., 2015) (see Table 2 and Fig.3).

The average concentration of  $^{238}\text{U}$  found in sediments of Oguta Lake, Nigeria (Isinkaye and Emelue, 2015); Lake Nasser, Egypt (Ibrahim et al., 1995); Lake Van (average upper and depth), Turkey (Erenturk et al., 2014); Altinkaya and Derbent Dam Lake, Turkey (Eroğlu and Kabadayi, 2013); Firtina River, Turkey (Kurnaz et al., 2007); Hunza, Gilgit and Indus Rivers, Pakistan (Qureshi et al., 2014); Tuomo River, Nigeria (Ugbede and Akpolile, 2019); Shango and Karnaphuli Rivers, Bangladesh (Chowdhury et al., 1999); China (Lu et al., 2008); and São Francisco River in Petrolina, Brazil (Da Silva and Da Silva Filho, 2019) are higher than the amount found in this study. Additionally,  $^{232}\text{Th}$  was found in sediments of Oguta Lake, Nigeria (Isinkaye and Emelue, 2015); Lake Van (average upper and depth), Turkey (Erenturk et al., 2014); Murath Dam Lake, Turkey (Kobyas et al., 2015); Palar River, India (Murugesan et al.,

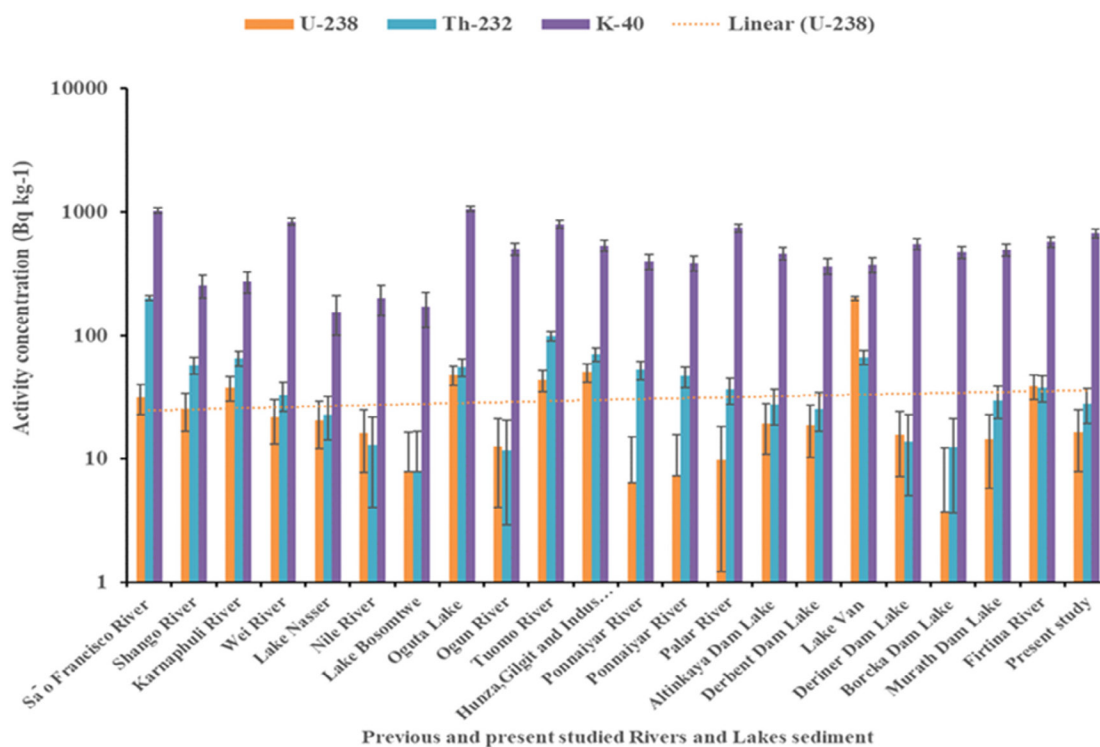


**Fig. 3.** Comparison of the average activity concentrations of  $^{238}\text{U}$ ,  $^{232}\text{Th}$ , and  $^{40}\text{K}$  of present study with sediments from rivers and lakes in various countries.

2015); Ponnaiyar River, India (Suresh et al., 2011; Ramasamy et al., 2011); Hunza, Gilgit and Indus Rivers, Pakistan (Qureshi et al., 2014); Tuomo River, Nigeria (Ugbede and Akpolile, 2019); Shango and Karnaphuli Rivers, Bangladesh (Chowdhury et al., 1999); China (Lu et al., 2008); and Sã o Francisco River in Petrolina, Brazil (Da Silva and Da Silva Filho, 2019) are higher than the amount found in this study, whereas  $^{40}\text{K}$  was found in sediments of Oguta Lake, Nigeria (Isinkaye and Emelue, 2015); Palar River, India (Murugesan et al., 2015); Tuomo River, Nigeria (Ugbede and Akpolile, 2019); and Wei River, China (Lu et al., 2008) are higher than the amount found in this study (see Table 2 and Fig.3). Because the concentrations of radioactive nuclides in nature are not uniform, it is essential to express radiological consequences using a single word that includes all of the fundamental radioactive nuclide hazards. Even if present in the same amount in any substance, the  $^{238}\text{U}$ ,  $^{232}\text{Th}$ , and  $^{40}\text{K}$  release differing gamma doses (Ugbede and Akpolile, 2019).

The levels of radium equivalent activity ( $Ra_{eq}$ ) range from  $51.40 \text{ Bq kg}^{-1}$  (sample SDS03) to  $175.51 \text{ Bq kg}^{-1}$  (sample SDS02), with an average of  $108.69 \text{ Bq kg}^{-1}$ , as calculated using  $equ^{ns}$ . 2 and presented in column 2 in Table 3. Radium equivalent activity ( $Ra_{eq}$ ) must have a minimum value of less than  $370 \text{ Bq kg}^{-1}$ , which is equivalent to a dose limit of  $1.00 \text{ mSv yr}^{-1}$  for the general public (ICRP,2007; UNSCEAR, 2008). The radium equivalent Activity ( $Ra_{eq}$ ) levels are significantly below the allowed limit of  $370 \text{ Bq kg}^{-1}$  for all of the sediment samples evaluated, including the average value. All human activities along the eastern coastline of Lake Hawassa and contamination of the environment around Lake Hawassa are safe.

The result of the external hazard index ( $H_{ex}$ ) was calculated using  $equ^{ns}$ . 3 ranges from 0.14 (SDS03) to 0.47 (SDS02), with an average of 0.29, as presented in column 3 in Table 3, respectively. In general, according to (ICRP, 1990), the average values are less than the allowed

**Table 3.** A summary of evaluated radiological hazard metrics found in Lake Hawassa sediments.

Sample code	Radiological hazard metrics					
	Raeq <sup>a</sup> (Bq kg <sup>-1</sup> )	Hex <sup>b</sup>	DRout <sup>c</sup> (nGy h <sup>-1</sup> )	AEDEout <sup>d</sup> (mSv yr <sup>-1</sup> )	ELCRout <sup>e</sup> (* 10 <sup>-3</sup> )	AGDE <sup>f</sup> (mSv yr <sup>-1</sup> )
SDS01	104.25	0.28	52.09	0.06	0.21	0.38
SDS02	175.51	0.47	82.7	0.10	0.35	0.59
SDS03	51.4	0.14	22.01	0.03	0.11	0.15
SDS04	115.2	0.31	56.4	0.07	0.25	0.41
SDS05	108.3	0.29	52.63	0.07	0.25	0.38
SDS06	103.33	0.28	51.73	0.07	0.21	0.38
SDS07	102.81	0.28	51.37	0.06	0.21	0.37
Average	108.69	0.29	52.7	0.07	0.23	0.38
Maximum	175.51	0.47	82.7	0.10	0.35	0.59
Minimum	51.4	0.14	22.01	0.03	0.11	0.15
Worldwide-recommended values (UNSCEAR, 2008)	370	1	59	0.07	0.29	0.3

<sup>a</sup> Radium equivalent activity; <sup>b</sup> External hazard index; <sup>c</sup> Outdoor absorbed dose rate; <sup>d</sup> Outdoor annual effective dose equivalent; <sup>e</sup> Outdoor excess lifetime cancer risk; <sup>f</sup> Annual gonadal dose equivalent

limits of 1, indicating that the radiological risk to human health along the eastern coastline of Lake Hawassa is insignificant and that it can be used freely for a variety of human activities.

Depending on the amounts of various radioactive elements in sediment samples, outdoor absorbed dose rate ( $D_{R_{out}}$ ) calculated using  $equ^{2.4}$  ranges from 22.01 to 82.70 nGy h<sup>-1</sup>, with an average value of 52.70 nGy h<sup>-1</sup>. The average value obtained is lower than the UNSCEAR (2008) (UNSCEAR, 2008) recommended maximum value of 59 nGy h<sup>-1</sup>. The higher outdoor absorbed dose ( $D_{R_{out}}$ ) value in the sample (SDS02) in the Lake Hawassa sediments was largely due to the high activity concentration found in <sup>232</sup>Th as presented in column 4 in Table 3. The percentages of the radionuclides <sup>238</sup>U, <sup>232</sup>Th, and <sup>40</sup>K that make up the total outdoor absorbed dose rates are 14.40 percent (53.10 nGy h<sup>-1</sup>), 32.28 percent (119.10 nGy h<sup>-1</sup>), and 53.32 percent (196.71 nGy h<sup>-1</sup>), respectively (see Fig.4).

The calculated outdoor annual effective dose ( $AEDE_{out}$ ) using  $equ^{2.5}$  ranges of 0.03 to 0.10 mSv yr<sup>-1</sup>, with average value of 0.07 mSv yr<sup>-1</sup>. This average outdoor annual effective dose is compatible to the 0.07 mSv yr<sup>-1</sup> worldwide average value (ICRP, 2007; UNSCEAR, 2008), yet it is still within the recommended allowed limits of 1.00 mSv yr<sup>-1</sup> for the public (ICRP, 2007; UNSCEAR, 2008) (see column 5 in Table 3). This suggests that the tested locality has low radiological contamination and, in terms of radon concentration and natural radioactivity, the Lake Hawassa eastern coastline is safe.

The calculated excess lifetime cancer risk (ELCR) using  $equ^{2.6}$  ranges from 0.11 x 10<sup>-3</sup> and 0.35 x 10<sup>-3</sup>, with average of 0.23 x 10<sup>-3</sup>. The average value is 12.61 percent lower than the 0.29 x 10<sup>-3</sup> worldwide-recommended value (see column 6 in Table 3). This  $ELCR_{out}$  value is a direct result of the external radiation exposure levels determined from the evaluated radionuclides in the sediments.

The calculated values of annual gonadal dose equivalent (AGDE) using  $equ^{2.7}$  ranges from 0.15 mSv yr<sup>-1</sup> and 0.59 mSv yr<sup>-1</sup>. The average value is 0.38 mSv yr<sup>-1</sup>, which is slightly higher than the UNSCEAR (2000) (UNSCEAR., 2000)-reported world average of 0.3 mSv yr<sup>-1</sup>, showing that the radionuclides found in the sediments of Lake Hawassa release low amounts of radiation, which has no consequence. Sample SDS02, on the other hand, has an AGDE value that is somewhat higher than the limit as presented in Table 3, column 7.

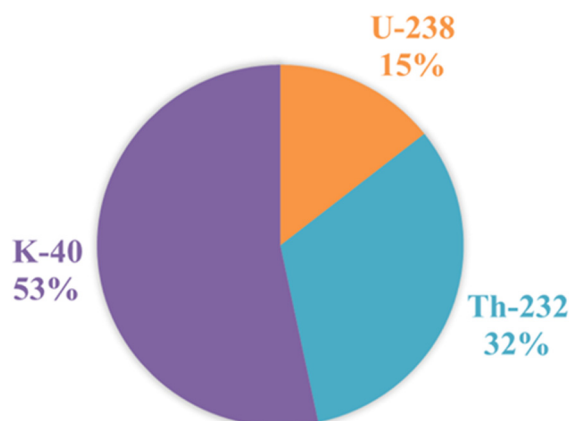


**Fig. 4.** Shows the makeup percentage contributions of the three natural radionuclides in sediments to the total outdoor absorbed dose rates.

#### *Statistical analysis and its descriptive statistics*

The statistical analysis was carried out using the IBM SPSS Statistics version 20 free computer software package for descriptive statistics, histograms, and Pearson's correlation analysis to depict the distributions and features of the three natural radionuclides ( $^{238}\text{U}$ ,  $^{232}\text{Th}$ , and  $^{40}\text{K}$ ) and their associated radiological hazard factors found in the sediments of Lake Hawassa's eastern coastline.

Descriptive statistics make it feasible to arrange or categorize raw scores in a way that makes them simpler to understand. By presenting the results in a table or graph, it is regularly possible to see the whole set of scores. Regardless of how many scores are in the data set, the mean provides a single descriptive figure for the whole set (Ravisankar et al., 2014).

Statistical metrics such as mean, standard deviation, variance, skewness, kurtosis, range, minimum, and maximum were computed, with the overall results presented in Table 4.

The frequency histogram and the corresponding distribution and feature curves for  $^{238}\text{U}$ ,  $^{232}\text{Th}$  and  $^{40}\text{K}$ , are shown in Fig.5, Fig.6, and Fig.7, respectively.

In descriptive statistics, "skewness" is a measure of how asymmetrically a distribution is

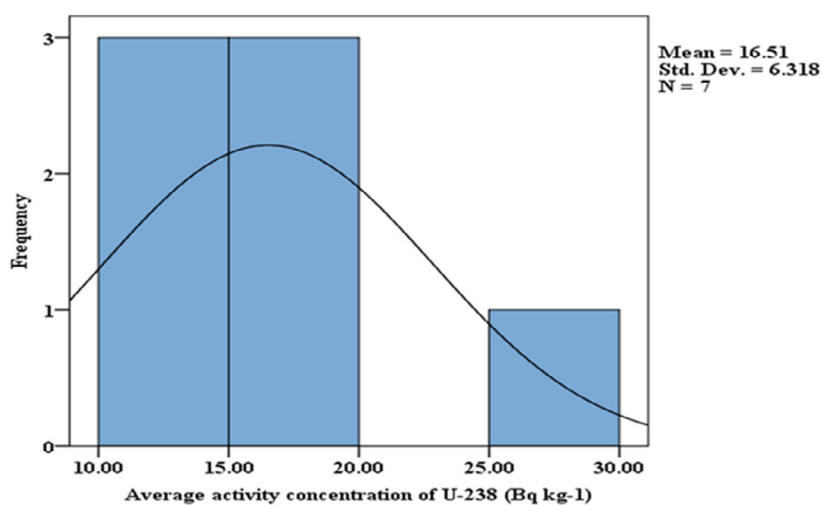


**Fig. 5.** Histograms represent the frequency distribution and features of the average activity concentration in  $^{238}\text{U}$  ( $\text{Bq kg}^{-1}$ ).

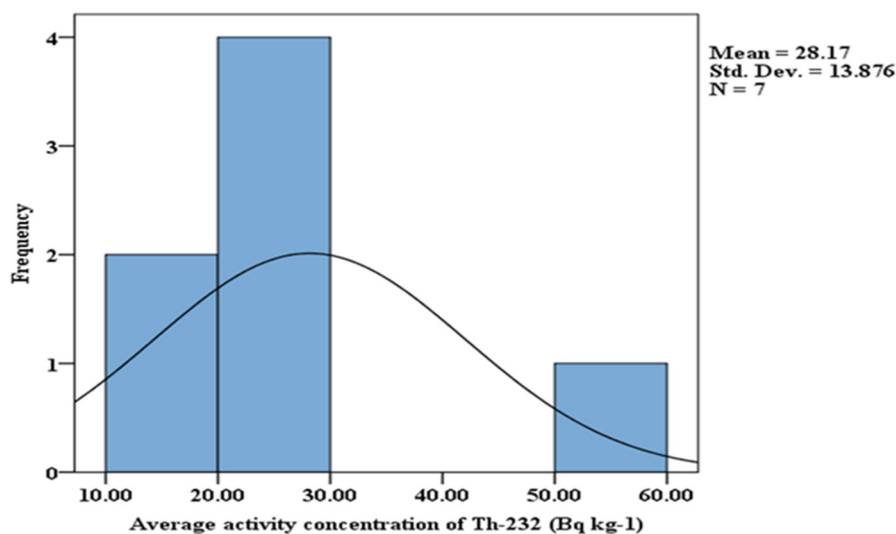


Fig. 6. Histograms represent the frequency distribution and features of the average activity concentration in <sup>232</sup>Th (Bq kg<sup>-1</sup>).

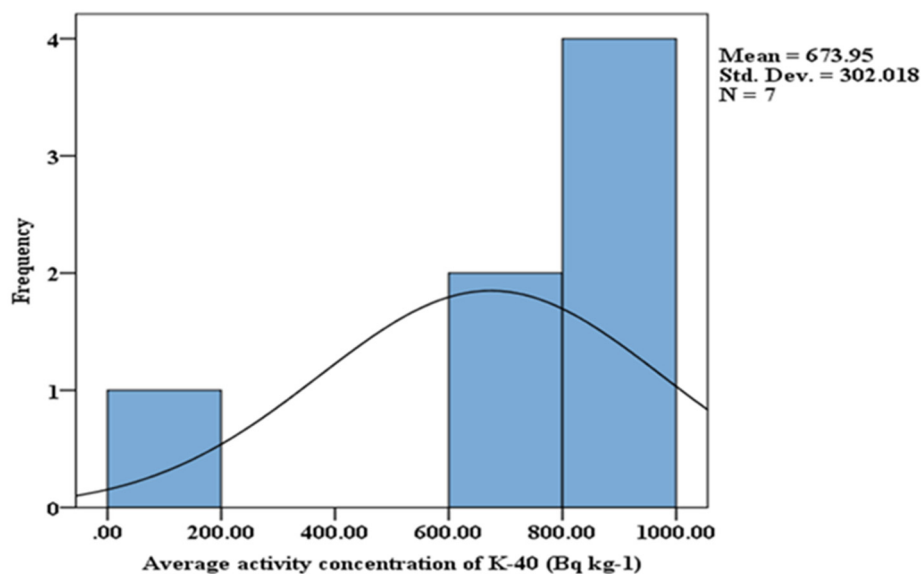


Fig. 7. Histograms represent the frequency distribution and features of the average activity concentration in <sup>40</sup>K (Bq kg<sup>-1</sup>).

centered on its mean. A distribution with an asymmetrically large tail toward higher positive values is said to have a positive skew. A distribution with an asymmetrically large tail extending toward greater negative values is indicated by negative skewness. Kurtosis is a metric for how peaked a real-valued random variable's probability distribution is. It describes how peaked or flat a distribution is compared to the normal distribution. A relatively peaked distribution is indicated by a positive kurtosis. A relatively flat distribution is assigned by negative kurtosis (SureshGandhi et al., 2014). The three naturally occurring radionuclides have positive kurtosis, which indicates a more peaked distribution as presented to Table 4 and Fig.5, Fig.6, and Fig.7. Only the radionuclide <sup>40</sup>K has a negative skewness, indicating an asymmetric lengthy tail extending toward greater negative values, according to Table 4 and Fig.7.

**Table 4.** Descriptive statistical behaviors of natural radionuclide variables of Lake Hawassa sediment samples.

Statistical metrics	U-238 ( Bq kg <sup>-1</sup> )	Th-232 ( Bq kg <sup>-1</sup> )	K-40 ( Bq kg <sup>-1</sup> )
Mean (AM)	16.5114	28.17	673.9486
Std. Deviation (SD)	6.31783	13.87634	302.01797
Variance	39.915	192.553	91214.853
Skewness	1.881	2.297	<b>-2.482</b>
Kurtosis	3.912	5.611	6.276
Range	18.03	39.6	827.21
Minimum	11.7	19.01	BDL
Maximum	29.73	58.61	827.21
Frequency distribution	Log-normal	Log-normal	Log-normal

The bold value represents only the negatively skewed value of <sup>40</sup>K.

In descriptive statistics, the distribution of data is represented graphically by a histogram. In terms of continuous variables, it predicts their probability distribution. Each radionuclide variable that was identified in sediment samples underwent a frequency distribution analysis; the results are represented as histograms in Fig.5, Fig.6, and Fig.7. The <sup>238</sup>U, <sup>232</sup>Th and <sup>40</sup>K graphs demonstrate the typical lognormal distribution of these radionuclides. However, there was some modality in <sup>40</sup>K. The radionuclide elements' modal characteristics show the range of minerals present in sediment samples (Ravisankar et al., 2014).

The linear Pearson correlation coefficient was computed as part of Pearson's correlation analysis to ascertain the mutual associations and strength of the correlations between pairs of variables. A significant positive correlation between the two variables suggests that the source and behavior of the variables are similar (Isinkaye and Emelue, 2015).

Table 5 summarizes the findings of the Pearson's correlation coefficients among all the calculated average activity concentrations of three-radioactive elements (<sup>238</sup>U, <sup>232</sup>Th, and <sup>40</sup>K) and their associated radiological hazard factors.

The table shows that all of the radiological hazard factors and the three-radioactive elements have a substantial positive correlation, i.e., that all three radionuclides are significantly responsible for the gamma radiation emission at the sample sites (Ravisankar et al., 2014). However, it was found that <sup>238</sup>U and <sup>232</sup>Th had positive, very strong correlations (R= 0.987), whereas <sup>40</sup>K only had positive, weak correlations with <sup>238</sup>U (R = 0.069) and <sup>232</sup>Th (R= 0.076).

The strong positive correlation between <sup>238</sup>U and <sup>232</sup>Th indicates that their source and behavior in the lake are similar; whereas the weak positive correlation <sup>40</sup>K with <sup>238</sup>U and <sup>232</sup>Th shows that, they may have the same source but exhibit different behaviors in the lake coastline environment (Isinkaye and Emelue, 2015).

The most of the assessed radiological hazard factors had substantial positive correlation coefficients, which shows a strong link between the pairs. Between Hex and Raeq, the correlation coefficient value (R = 1.000) exists, denoting a complete linear correlation and an indication of togetherness. Radium equivalent activity (Raeq), the external hazard index (Hex), and outdoor annual effective dose equivalent (AEDEout) all have very comparable correlation coefficient values (R = 0.978). Additionally, the external hazard index (Hex), radium equivalent activity (Raeq), and annual gonadal dose equivalent (AGDE) all have very similar correlation analysis values (R = 0.989). Outdoor excess lifetime cancer risk (ELCRout) and the external hazard index (Hex) have incredibly strong correlation values (R = 0.984) as presented in Table 5. The radiological hazard factors ELCRout and AGDE are linearly related to DRout with R<sup>2</sup> = 0.962 and 0.998, respectively, as shown in Fig.8 and Fig.9.

**Table 5.** Pearson correlation coefficients were analyzed between activity concentrations of three natural radioactive elements and radiological hazard variables in sediment samples.

Radiological hazard variables	U-238	Th-232	K-40	Raeq	Hex	DRout	AEDEout	ELCRout	AGDE
U-238	1								
Th-232	0.987*	1							
K-40	0.069	0.076	1						
Raeq	0.759	0.769	0.696	1					
Hex	0.754	0.764	0.700	<b>1.000</b>	1				
DRout	0.686	0.695	0.769	0.994*	0.995*	1			
AEDEout	0.702	0.688	0.745	0.978*	0.978*	0.982*	1		
ELCRout	0.763	0.746	0.690	0.985*	0.984*	0.981*	0.980*	1	
AGDE	0.657	0.665	0.794	0.989*	0.989*	0.999*	0.983*	0.977*	1

The bolded value represents the perfect positive correlation.  
 All one-tailed values show a very strong correlation among variables.

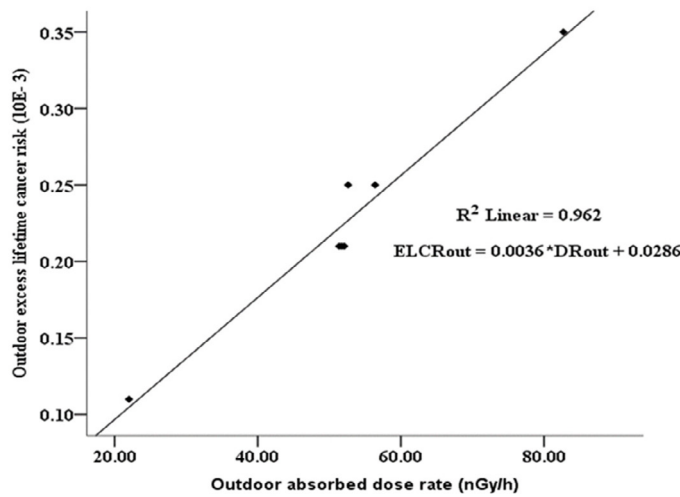


**Fig. 8.** Shows the very high positive association between the outdoor absorbed dose rates (DRout) and outdoor excess lifetime cancer risk (ELCRout) for the study location.

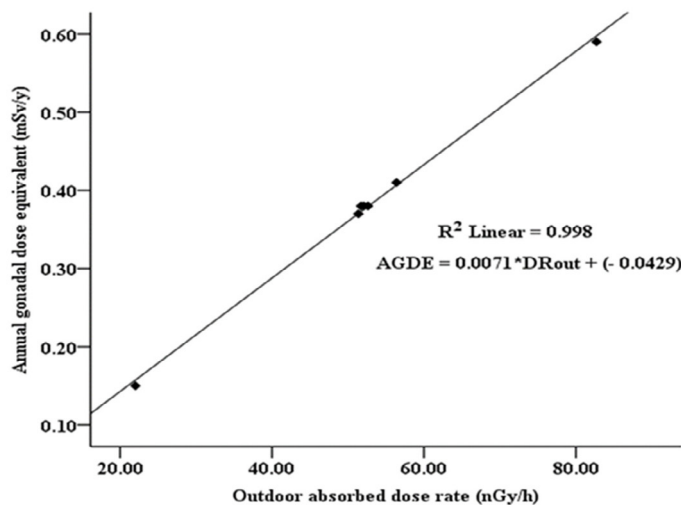


**Fig. 9.** Shows the very high positive association between the outdoor absorbed dose rates (DRout) and annual gonadal dose equivalent (AGDE) for the study location.



### *Geographical distribution of radioactivity levels in the ratios $^{232}\text{Th}/^{238}\text{U}$ , $^{40}\text{K}/^{238}\text{U}$ , and $^{40}\text{K}/^{232}\text{Th}$*

The  $^{232}\text{Th}/^{238}\text{U}$  ratio is a good indicator of the relative concentration or reduction of radioisotopes (Örgün et al., 2007). According to estimations of the  $^{232}\text{Th}/^{238}\text{U}$  activity ratio, the  $^{232}\text{Th}$  activity concentrations in the analyzed sediment samples are on average about 1.67 times greater than the  $^{238}\text{U}$  activity concentrations. The highest  $^{232}\text{Th}/^{238}\text{U}$  ratio was observed in SDS02 (1.97) site location of latitude (N)  $7^{\circ} 00' 52.83''$  and longitude (E)  $38^{\circ} 27' 50.86''$ . This demonstrated that  $^{232}\text{Th}$  ( $58.61 \text{ Bq kg}^{-1}$ ) exists in substantially higher amounts than  $^{238}\text{U}$  ( $29.73 \text{ Bq kg}^{-1}$ ). This might be because of the loamy sediments at site SDS02, which contain a significant quantity of  $^{232}\text{Th}$ .  $^{232}\text{Th}/^{238}\text{U}$  ratios over this range are present in all sediment samples from the investigation area.  $^{232}\text{Th}/^{238}\text{U}$  ratios are mostly within this xenolith zircon extend the previously reported range to 0.3-2 for the studied location samples. Consequently, the present investigation supports the strong likelihood that zircon is found in the sediments. This may indicate that the study's findings on zircon's highest level of presence in sediments (El-Gamal et al., 2007; SureshGandhi et al., 2014).

The  $^{40}\text{K}/^{232}\text{Th}$  ratio is significant and changes depending on the type of clay material.  $^{232}\text{Th}$  and  $^{40}\text{K}$  react differently to weathering than one another. In contrast to  $^{232}\text{Th}$ , which tends to stay,  $^{40}\text{K}$  is more soluble and easily transported away in water. Higher values of  $^{40}\text{K}/^{238}\text{U}$  and  $^{40}\text{K}/^{232}\text{Th}$  at the present study's sites SDS07 ( $69.67 \text{ Bq kg}^{-1}$ ) and SDS06 ( $43.51 \text{ Bq kg}^{-1}$ ), respectively, may suggest that clay is found there. The  $^{40}\text{K}/^{238}\text{U}$  and  $^{40}\text{K}/^{232}\text{Th}$  activity ratios do not show any clear trend and have a very weak positive correlation (Murugesan et al., 2011).

## CONCLUSIONS

Gamma-ray spectrometry (HPGe detector) was used in this investigation to measure average activity concentrations due to naturally occurring radionuclides ( $^{238}\text{U}$ ,  $^{232}\text{Th}$ , and  $^{40}\text{K}$ ) and assess the associated radiological hazard risk levels in surface sediment samples collected from seven different sites covering 40% of the eastern coastline of Lake Hawassa. The average concentrations for  $^{238}\text{U}$ ,  $^{232}\text{Th}$ , and  $^{40}\text{K}$  are 16.51, 28.17, and 673.95  $\text{Bq kg}^{-1}$ , respectively. The average activity concentrations of  $^{238}\text{U}$  and  $^{232}\text{Th}$  were lower than the worldwide-recommended values, but  $^{40}\text{K}$  was higher than the worldwide-recommended safe value reported by UNSCEAR in 2008, and the results of this investigation were compared with other studies of different parts of the world. Furthermore, the calculated average radiological hazard factors (radium equivalent, hazard index (external hazard index ( $H_{ex}$ )), excess lifetime cancer risk, absorbed dose rate, annual effective dose equivalent, and annual gonadal dose equivalent) to assess the possible hazard risk of radiation exposure to health in sediment samples are lower than the worldwide recommended safe values reported by UNSCEAR, 2008. As a result, insignificant radiation health risks or environmental risks were posed to people who regularly engage in diverse activities such as recreation, fishing, fish sales, eating raw fish, washing clothes, farming, and taking a bath along the eastern coastline of Lake Hawassa. This investigation is regarded as the first carried out on natural radioactivity levels in this area, so it appears as an essential radiometric baseline for ongoing environmental monitoring programs and a data reference for future investigations in the study area.

## ACKNOWLEDGMENTS

The authors are grateful to Mr. Eshetu Tilahun and his colleagues for their help in analyzing the samples using gamma-ray spectrometry (HPGe detector) and to the chairperson of the Physics department at Addis Ababa University for his interest in the present project.

## FUNDING STATEMENT

The present research did not received any financial support

## CONFLICT OF INTEREST

The authors declare that there is not any conflict of interests regarding the publication of this manuscript.

## LIFE SCIENCE REPORTING

No life science threat was practiced in the research.

## DATA AVAILABILITY STATEMENT

The data that support the findings of this investigation are available in the “Zenodo” repository at <https://doi.org/10.5281/zenodo.7567710>.

## REFERENCES

- Beretka, J., & Mathew, P. J. (1985). Natural radioactivity of australian building materials, industrial wastes and by-products. *Health Phys.*, 48(1), 87-95. <https://doi.org/10.1097/00004032-198501000-00007>.
- Botwe, B. O., Schirone, A., Delbono, I., Barsanti, M., Delfanti, R., Kelderman, P., . . . Lens, P. N. (2016). Radioactivity concentrations and their radiological significance in sediments of the Tema Harbour (Greater Accra, Ghana). *J. Radiat. Res. Appl. Sci.*, 10(1), 63-71. <https://doi.org/10.1016/j.jrras.2016.12.002>.
- Chowdhury, M. I., Alam, M. N., & Hazari, S. K. (1999). Distribution of radionuclides in the river sediments and coastal soils of Chittagong, Bangladesh and evaluation of the radiation hazard. *Appl. Radiat. Isot.*, 51(6), 747-755. [https://doi.org/10.1016/S0969-8043\(99\)00098-6](https://doi.org/10.1016/S0969-8043(99)00098-6).
- Da Silva, C. M., & Da Silva Filho, C. A. (2019). Natural radionuclides in water and sediments of the São Francisco River in Petrolina, Brazil. *Int. J. Low Radiat.*, 11(2), 89. <https://doi.org/10.1504/ijlr.2019.10024897>.
- Darko, G., Ansah, E., Faanu, A., & Azanu, D. (2017). Natural radioactivity and heavy metal distribution in reservoirs in Ghana. *Pollution*, 3(2), 225-241. <https://doi.org/10.7508/pj.2017.02.006>.
- Darwish, D., Abul-Nasr, K., & El-Khayatt, A. (2015). The assessment of natural radioactivity and its associated radiological hazards and dose parameters in granite samples from South Sinai, Egypt. *J. Radiat. Res. Appl. Sci.*, 8(1), 17-25. <https://doi.org/10.1016/j.jrras.2014.10.003>.
- El Mamoney, M. H., & Khater, A. E. (2004). Environmental characterization and radio-ecological impacts of non-nuclear industries on the Red Sea coast. *J. Environ. Radioact.*, 73(2), 151-168. <https://doi.org/10.1016/j.jenvrad.2003.08.008>.
- El-Gamal, A., Nasr, S., & El-Taher, A. (2007). Study of the spatial distribution of natural radioactivity in the upper Egypt Nile River sediments. *Radiat. Meas.*, 42(3), 457-465. <https://doi.org/10.1016/j.radmeas.2007.02.054>.
- Erenturk, S., Yusan, S., Turkozu, D. A., Camtakan, Z., Olgen, M. K., Aslani, M. A., . . . Isik, M. A. (2014). Spatial distribution and risk assessment of radioactivity and heavy metal levels of sediment, surface water and fish samples from Lake Van, Turkey. *J. Radioanal. Nucl. Chem.*, 300(3), 919-931. <https://doi.org/10.1007/s10967-014-3042-0>.
- Eroğlu, H., & Kabadayi, Ö. (2013). Natural radioactivity levels in lake sediment samples. *Radiat. Prot. Dosim.*, 156(3), 331-335. <https://doi.org/10.1093/rpd/nct071>.
- Fares, S. (2017). Measurements of natural radioactivity level in black sand and sediment samples of the Tamsah Lake beach in Suez Canal region in Egypt. *J. Radiat. Res. Appl. Sci.*, 10(3), 194-203. <https://doi.org/10.1016/j.jrras.2017.04.007>.

- Hameed, P. S., Pillai, G. S., Satheeshkumar, G., & Mathiyarasu, R. (2014). Measurement of gamma radiation from rocks used as building material in Tiruchirappalli district, Tamil Nadu, India. *J. Radioanal. Nucl. Chem.*, 300(3), 1081-1088. <https://doi.org/10.1007/s10967-014-3033-1>.
- Ibrahim, M. N., Shawkay, S., & Amer, H. (1995). Radioactivity levels in lake Nasser sediments. *Appl. Radiat. Isot.*, 46(5), 297-299.
- ICRP. (1990). The 1990 Recommendations of the International Commission on Radiological Protection. Oxford, UK: ICRP Publication 60. *Annals of the ICRP*. 21(1-3).
- ICRP, .. (2007). The 2007 Recommendations of the International Commission on Radiological Protection: *Annals of the ICRP publication* 103. 37(2-4).
- ICRP. (2008). Radiation Dose to Patients from Radiopharmaceuticals. Addendum 3 to ICRP Publication 53. ICRP Publication 106. 38(1-2).
- Isinkaye, M., & Emelue, H. (2015). Natural radioactivity measurements and evaluation of radiological hazards in sediment of Oguta Lake, South East Nigeria. *J. Radiat. Res. Appl. Sci.*, 8(3), 459-469. <https://doi.org/10.1016/j.jrras.2015.05.001>.
- Jibiri, N. N., & Okeyode, I. C. (2012). Evaluation of radiological hazards in the sediments of Ogun river, South-Western Nigeria. *Radiat. Phys. Chem.*, 81(2), 103-112. <https://doi.org/10.1016/j.radphyschem.2011.10.002>.
- Jibiri, N., & Okeyode, I. (2011). Activity concentrations of natural radionuclides in the sediments of Ogun River, southwestern Nigeria. *Radiat. Prot. Dosim.*, 147(4), 555-564. <https://doi.org/10.1093/rpd/ncq579>.
- Karahan, G., & Bayulken, A. (2000). Assessment of gamma dose rates around Istanbul (Turkey). *J. Environ. Radioact.*, 47(2), 213-221. [https://doi.org/10.1016/S0265-931X\(99\)00034-X](https://doi.org/10.1016/S0265-931X(99)00034-X).
- Khater, A. E., Ebaid, Y. Y., & El-Mongy, S. A. (2005). Distribution pattern of natural radionuclides in Lake Nasser bottom sediments. *Int. Congr. Ser.*, 1276, 405-406. <https://doi.org/10.1016/j.ics.2004.11.112>.
- Koby, Y., Taşkın, H., Yeşilkanat, C. M., Varinlioğlu, A., & Korcak, S. (2015). Natural and artificial radioactivity assessment of dam lakes sediments in Çoruh River, Turkey. *J. Radioanal. Nucl. Chem.*, 303(1), 287-295. <https://doi.org/10.1007/s10967-014-3420-7>.
- Kurnaz, A., Küçükömeroğlu, B., Keser, R., Okumusoglu, N. T., Korkmaz, F., Karahan, G., & Çevik, U. (2007). Determination of radioactivity levels and hazards of soil and sediment samples in Fırtına Valley (Rize, Turkey). *Appl. Radiat. Isot.*, 65(11), 1281-1289. <https://doi.org/10.1016/j.apradiso.2007.06.001>.
- Lu, X., Zhang, X., & Wang, F. (2008). Natural radioactivity in sediment of Wei River, China. *Environ. Geol.*, 53(7), 1475-1481. <https://doi.org/10.1007/s00254-007-0756-0>.
- Menberu, Z., Mogesse, B., & Reddythota, D. (2021). Regional Studies Assessment of morphometric changes in Lake Hawassa by using surface and bathymetric maps. *J. Hydrol. Reg. Stud.*, 36(June), 100852. <https://doi.org/10.1016/j.ejrh.2021.100852>.
- Morsy, Z., El-Wahab, M. A., & El-Faramawy, N. (2012). Determination of natural radioactive elements in Abo Zaabal, Egypt by means of gamma spectroscopy. *Ann. Nucl. Energy*, 44(September 2020), 8-11. <https://doi.org/10.1016/j.anucene.2012.01.003>.
- Mulugeta, D. B., David, H.-C., Ruth E., M., & Cryton, Z. (2021). Building foundations for source-to-sea management: the case of sediment management in the Lake Hawassa sub-basin of the Ethiopian Rift Valley. *Water Int.*, 46(2), 138-156. <https://doi.org/10.1080/02508060.2021.1889868>.
- Murugesan, S., Mullainathan, S., Ramasamy, V., & Meenakshisundaram, V. (2011). Radioactivity and radiation hazard assessment of Cauvery River, Tamilnadu, India. *Iran. J. Radiat. Res.*, 8(4), 211-222.
- Murugesan, S., Mullainathan, S., & Ramasamy, V. (2015). Natural radioactivity and hazardous index of major South Indian river sediments. *Int. J. Low Radiat.*, 10(1), 14-33. <https://doi.org/10.1504/IJLR.2015.071761>.
- Onjefu, A. S., Taole H., S., Kgabi A., N., Grant, C., & Antoine, J. (2017). Assessment of natural radionuclide distribution in shore sediment samples collected from the North Dune beach, Henties Bay, Namibia. *J. Radiat. Res. Appl. Sci.*, 10(4), 301-306. <https://doi.org/10.1016/j.jrras.2017.07.003>.
- Orgun, Y., Altınsoy, N., Sahin, S., Gungor, Y., Gultekin, A., Karahan, G., & Karacık, Z. (2007). Natural and anthropogenic radionuclides in rocks and beach sands from Ezine region (C- anakkale), Western Anatolia, Turkey. *Appl. Radiat. Isot.*, 65, 739-747. <https://doi.org/10.1016/j.apradiso.2006.06.011>.
- Powell, B. A., Hughes, L. D., Soreefan, A. M., Falta, D., Wall, M., & Devol, T. A. (2007). Elevated concentrations of primordial radionuclides in sediments from the Reedy River and surrounding creeks in Simpsonville, South Carolina. *J. Environ. Radioact.*, 94, 121-128. <https://doi.org/10.1016/j.jrras.2007.06.001>.

- jenvrad.2006.12.013.
- Qureshi, A. A., Tariq, S., Din, K. U., Manzoor, S., Calligaris, C., & Waheed, A. (2014). Evaluation of excessive lifetime cancer risk due to natural radioactivity in the rivers sediments of Northern Pakistan. *J. Radiat. Res. Appl. Sci.*, 7(4), 438-447. <https://doi.org/10.1016/j.jrras.2014.07.008>.
- Ramasamy, V., Sundarrajan, M., Suresh, G., Paramasivam, K., & Meenakshisundaram, V. (2014). Role of light and heavy minerals on natural radioactivity level of high background radiation area, Kerala, India. *Appl. Radiat. Isot.*, 85, 1-10. <https://doi.org/10.1016/j.apradiso.2013.11.119>.
- Ramasamy, V., Suresh, G., Meenakshisundaram, V., & Ponnusamy, V. (2011). Horizontal and vertical characterization of radionuclides and minerals in river sediments. *Appl. Radiat. Isot.*, 69(1), 184-195. <https://doi.org/10.1016/j.apradiso.2010.07.020>.
- Ravisankar, R., Sivakumar, S., Chandrasekaran, A., Prince Prakash Jebakumar, J., Vijayalakshmi, I., Vijayagopal, P., & Venkatraman, B. (2014). Spatial distribution of gamma radioactivity levels and radiological hazard indices in the East Coastal sediments of Tamilnadu, India with statistical approach. *Radiat. Phys. Chem.*, 103, 89-98. <https://doi.org/10.1016/j.radphyschem.2014.05.037>.
- Semaria Moga, L., Jens, T., & Mihret, D. (2021). Assessing the Water Quality of Lake Hawassa Ethiopia-Trophic State and Suitability for Anthropogenic Uses—Applying Common Water Quality Indices Assessing the Water Quality of Lake Hawassa Ethiopia — Trophic State and Suitability for Anthropogenic Uses. *Int. J. Environ. Res. Public Health*, 18(August), 8904. <https://doi.org/10.3390/ijerph18178904>.
- Shetty, P., & Narayana, Y. (2010). Variation of radiation level and radionuclide enrichment in high background area. *J. Environ. Radioact.*, 101(12), 1043-1047. <http://doi.org/10.1016/j.jenvrad.2010.08.003>.
- Suresh, G., Ramasamy, V., Meenakshisundaram, V., Venkatachalapathy, R., & Ponnusamy, V. (2011). A relationship between the natural radioactivity and mineralogical composition of the Ponnaiyar river sediments, India. *J. Environ. Radioact.*, 102(4), 370-377. <https://doi.org/10.1016/j.jenvrad.2011.02.003>.
- SureshGandhi, M., Ravisankar, R., Rajalakshmi, A., Sivakumar, S., Chandrasekaran, A., & Pream Anand, D. (2014). Measurements of natural gamma radiation in beach sediments of north east coast of Tamilnadu, India by gamma ray spectrometry with multivariate statistical approach. *J. Radiat. Res. Appl. Sci.*, 7(1), 7-17. <https://doi.org/10.1016/j.jrras.2013.11.001>.
- Tarekegn, W., & Seyoum, M. (2020). Effects of anthropogenic activities on macroinvertebrate assemblages in the littoral zone of Lake Hawassa , a tropical Rift Valley Lake in Ethiopia. *Lakes Reserv.: Res. Manag.* (April 2019), 1-11. <https://doi.org/10.1111/lre.12303>.
- Tzortzis, M., Svoukis, E., & Tsertos, H. (2004). A comprehensive study of natural gamma radioactivity levels and associated dose rates from surface soils in Cyprus. *Radiat. Prot. Dosim.*, 109(3), 217-224. <https://doi.org/10.1093/rpd/nch300>.
- Ugbede, F., & Akpolile, A. (2019). Determination of Specific Activity of <sup>238</sup>U, <sup>232</sup>Th and <sup>40</sup>K and Radiological Hazard. *J. Appl. Sci. Environ. Manage.*, 23(4), 727-733. <https://doi.org/10.4314/jasem.v23i4.24>.
- Ugbede, F., & Benson, I. (2018). Assessment of outdoor radiation levels and radiological health hazards in Emene Industrial Layout of Enugu State, Nigeria. *Int. J. Phys. Sci.*, 13(20), 265-272. <https://doi.org/10.5897/ijps2018.4763>.
- UNSCEAR. (1993). *Sources and effects of ionizing radiation: UNSCEAR 1993 report to the General Assembly*. New York, NY: United Nations.
- UNSCEAR, .. (2008). *Sources and Effects of Ionizing Radiation, Report to the General Assembly, with Scientific Annexes*. New York: United Nations.
- UNSCEAR. (2000). *Sources and Effects of Ionizing Radiation: United Nations Scientific Committee on the Effects of Atomic Radiation UNSCEAR 2000 Report to the General Assembly, with Scientific*. New York: UNSCEAR 2000 Report.